JVI Journals.ASM.org

Chronic Administration of Δ^9-Tetrahydrocannabinol Induces Intestinal Anti-Inflammatory MicroRNA Expression during Acute Simian Immunodeficiency Virus Infection of Rhesus Macaques

Lawrance C. Chandra,[a] Vinay Kumar,[a] Workineh Torben,[a] Curtis Vande Stouwe,[c] Peter Winsauer,[b,d] Angela Amedee,[b,e] Patricia E. Molina,[b,c] Mahesh Mohan[a]

Division of Comparative Pathology, Tulane National Primate Research Center, Covington, Louisiana, USA[a]; LSUHSC Alcohol and Drug Abuse Center, New Orleans, Louisiana, USA[b]; Departments of Physiology,[c] Pharmacology,[d] and Microbiology,[e] Louisiana State University Health Sciences Center, New Orleans, Louisiana, USA

ABSTRACT

Recreational and medical use of cannabis among human immunodeficiency virus (HIV)-infected individuals has increased in recent years. In simian immunodeficiency virus (SIV)-infected macaques, chronic administration of Δ^9-tetrahydrocannabinol (Δ^9-THC) inhibited viral replication and intestinal inflammation and slowed disease progression. Persistent gastrointestinal disease/inflammation has been proposed to facilitate microbial translocation and systemic immune activation and promote disease progression. Cannabinoids including Δ^9-THC attenuated intestinal inflammation in mouse colitis models and SIV-infected rhesus macaques. To determine if the anti-inflammatory effects of Δ^9-THC involved differential microRNA (miRNA) modulation, we profiled miRNA expression at 14, 30, and 60 days postinfection (days p.i.) in the intestine of uninfected macaques receiving Δ^9-THC ($n = 3$) and SIV-infected macaques administered either vehicle (VEH/SIV; $n = 4$) or THC (THC/SIV; $n = 4$). Chronic Δ^9-THC administration to uninfected macaques significantly and positively modulated intestinal miRNA expression by increasing the total number of differentially expressed miRNAs from 14 to 60 days p.i. At 60 days p.i., ~28% of miRNAs showed decreased expression in the VEH/SIV group compared to none showing decrease in the THC/SIV group. Furthermore, compared to the VEH/SIV group, THC selectively upregulated the expression of miR-10a, miR-24, miR-99b, miR-145, miR-149, and miR-187, previously been shown to target proinflammatory molecules. NOX4, a potent reactive oxygen species generator, was confirmed as a direct miR-99b target. A significant increase in NOX4$^+$ crypt epithelial cells was detected in VEH/SIV macaques compared to the THC/SIV group. We speculate that miR-99b-mediated NOX4 downregulation may protect the intestinal epithelium from oxidative stress-induced damage. These results support a role for differential miRNA induction in THC-mediated suppression of intestinal inflammation. Whether similar miRNA modulation occurs in other tissues requires further investigation.

IMPORTANCE

Gastrointestinal (GI) tract disease/inflammation is a hallmark of HIV/SIV infection. Previously, we showed that chronic treatment of SIV-infected macaques with Δ^9-tetrahydrocannabinol (Δ^9-THC) increased survival and decreased viral replication and infection-induced gastrointestinal inflammation. Here, we show that chronic THC administration to SIV-infected macaques induced an anti-inflammatory microRNA expression profile in the intestine at 60 days p.i. These included several miRNAs bioinformatically predicted to directly target CXCL12, a chemokine known to regulate lymphocyte and macrophage trafficking into the intestine. Specifically, miR-99b was significantly upregulated in THC-treated SIV-infected macaques and confirmed to directly target NADPH oxidase 4 (NOX4), a reactive oxygen species generator known to damage intestinal epithelial cells. Elevated miR-99b expression was associated with a significantly decreased number of NOX4$^+$ epithelial cells in the intestines of THC-treated SIV-infected macaques. Overall, our results show that selective upregulation of anti-inflammatory miRNA expression contributes to THC-mediated suppression of gastrointestinal inflammation and maintenance of intestinal homeostasis.

Increasing evidence suggests that both the natural and synthetic forms of Δ^9-tetrahydrocannabinol (e.g., Dronabinol) stimulate appetite, increase weight gain, and improve the overall quality of life of HIV-infected patients (1, 2). Recent advances in our understanding of its pharmacology and the role of the major cannabinoid receptor subtypes have resulted in the elucidation of the cannabinoid's additional biomedical effects, particularly its capacity for modulating the immune and inflammatory responses (3–5). This is evident from recent reports demonstrating the anti-inflammatory properties of cannabinoids in numerous chronic inflammatory disorders, such as inflammatory bowel disease, arthritis, autoimmune disorders, multiple sclerosis, etc. (6–8). These findings are exciting and have created renewed interest in determining the therapeutic potential of cannabinoids, especially in modulating the immune/inflammatory responses in human immunodeficiency virus (HIV)-infected individuals. Delineating the effects of cannabinoids in the HIV-infected population is difficult and challenging due to the effects of various confounding factors such as multidrug usage, nutritional status, and the dynamic nature of the disease process. Consequently, the simian immunodeficiency virus (SIV)-infected rhesus macaque model is beneficial in eliminating these variables, and our previous studies have clearly shown that chronic Δ^9-THC treatment attenuated viral load and tissue inflammation, resulting in a significant de-

crease in male rhesus macaque morbidity and mortality from SIV infection (9–11).

The gastrointestinal (GI) immune system, the largest lymphoid organ, contains an abundant population of activated CCR5/CD4$^+$ memory T cells and is a major target site for HIV/SIV replication and dissemination (12–15). GI disease/inflammation, largely driven by proinflammatory cytokine production in response to viral replication, is a hallmark feature of HIV/SIV infection (16–18). Further, inflammation-induced disruption of the intestinal epithelial barrier has also been proposed to facilitate the translocation of luminal bacteria and their products, which drives disease progression through localized and systemic immune activation (19). Hence, there is a great need to identify the mechanisms that curtail viral replication, immune activation, and chronic persistent inflammation in HIV-infected individuals. In this context, the potential for cannabinoids to modulate gastrointestinal function and inflammatory responses is strengthened by the presence of cannabinoid receptors in the myenteric and submucosal plexus, including immune cells (B cells, NK cells, and macrophages) residing in the lamina propria (20). Accordingly, several studies have confirmed the ability of cannabinoids to significantly alleviate the severity of colitis and to normalize intestinal motility in experimental animal models of inflammatory bowel and Crohn's disease patients (21, 22). Further, and more importantly, increased expression of the cannabinoid type-2 receptor (CB2) has been associated with anti-inflammatory effects in the gastrointestinal tract (18, 19). Consistent with these findings, we recently showed that chronic THC administration in SIV-infected rhesus macaques was associated with increased survival of T-cell populations and considerable protection of the GI tract from crypt cell apoptosis and infection-related inflammation (23). In addition, cannabinoids also suppressed HIV replication in *in vitro*-cultured macrophages acting predominantly through CB2 receptors (24).

While the effects of the cannabinoids on inflammation and viral replication have been reported by others and confirmed by our recent macaque studies (9, 23), mechanistic studies to elucidate these protective effects are needed. Several recent reports have linked altered microRNA (miRNA) expression, a newly identified class of noncoding RNAs that function to regulate gene expression to alcohol, morphine, and cocaine addiction (25–29). Although not related to HIV infection, these studies clearly suggest that drugs of abuse can alter miRNA expression to produce epigenetic effects. These findings also suggest that the protective effects of cannabinoids may also be mediated by similar regulatory factors/mechanisms (epigenetic) that need to be further investigated and identified, especially as they relate to HIV infection. For instance, several *in vitro* studies have shown altered miRNA expression in response to HIV infection (30–34), and recent miRNA profiling studies performed on brain (35) and plasma samples (36) provide strong evidence of their dysregulation during SIV infection. In addition, we recently reported miR-190b to be significantly upregulated in the intestine at all stages of SIV infection (37) and that viral replication rather than infection-related inflammatory responses induced miR-190b upregulation (37). Further, we also confirmed MTMR6, a PIP3 phosphatase and an inhibitor of CD4$^+$ T cell proliferation and activation, to be a direct miR-190b target (37).

Although the GI tract/immune system is the major site for HIV replication and pathogenesis, little is known about the effect of THC on the GI tract during acute HIV/SIV infection. Moreover, the extent to which the cannabinoids (both exogenous and endogenous) exert their anti-inflammatory effects by modulating the expression of specific miRNAs is unknown. Therefore, we hypothesized that THC may modulate the early events of HIV/SIV pathogenesis in the GI tract by altering intestinal miRNA expression, particularly those miRNAs targeting proinflammatory mediators. In the present study, we profiled miRNA expression in duodenal biopsy specimens/tissues collected from THC-treated uninfected and SIV-infected rhesus macaques using the TaqMan OpenArray human microRNA platform. Our results show that THC alone induced significant alterations in miRNA expression in the GI tract. Interestingly, compared to what was observed in the VEH/SIV group, THC administration to SIV-infected macaques resulted in the selective upregulation of a cluster of six miRNAs previously shown to exert anti-inflammatory effects. Among the six, we characterized the functional relevance of miR-99b and found its expression to be significantly increased in THC-treated SIV-infected macaques. We also found that a potent reactive oxygen species (ROS) generator, NADPH oxidase 4 (NOX4), was a direct target of miR-99b. Finally, we show that elevated miR-99b expression in the duodenum of THC/SIV macaques was accompanied by a significantly reduced number of NOX4$^+$ crypt epithelial cells.

Received 17 June 2014 **Accepted** 30 October 2014

Accepted manuscript posted online 5 November 2014

Citation Chandra LC, Kumar V, Torben W, Stouwe CV, Winsauer P, Amedee A, Molina PE, Mohan M. 2015. Chronic administration of Δ^9-tetrahydrocannabinol induces intestinal anti-inflammatory microRNA expression during acute simian immunodeficiency virus infection of rhesus macaques. J Virol 89:1168–1181. doi:10.1128/JVI.01754-14.

Editor: R. W. Doms

Address correspondence to Mahesh Mohan, mmohan@tulane.edu.

Supplemental material for this article may be found at http://dx.doi.org/10.1128/JVI.01754-14.

doi:10.1128/JVI.01754-14

MATERIALS AND METHODS

Animal care, ethics, and experimental procedures. All experiments using rhesus macaques were approved by the Tulane and LSUHSC Institutional Animal Care and Use Committee (Protocol No-3581). The Tulane National Primate Research Center (TNPRC) is an Association for Assessment and Accreditation of Laboratory Animal Care International accredited facility (AAALAC number 000594). The NIH Office of Laboratory Animal Welfare assurance number for the TNPRC is A3071-01. All clinical procedures, including administration of anesthesia and analgesics, were carried out under the direction of a laboratory animal veterinarian. Animals were anesthetized with ketamine hydrochloride for blood collection procedures. Intestinal pinch biopsies were performed by laboratory animal veterinarians. Animals were preanesthetized with ketamine hydrochloride, acepromazine, and glycopyrolate, intubated, and maintained on a mixture of isoflurane and oxygen. All possible measures were taken to minimize discomfort of all the animals used in this study. Tulane University complies with NIH policy on animal welfare, the Animal Welfare Act, and all other applicable federal, state and local laws.

Animal model and experimental design. Twelve age- and weight-matched male Indian rhesus macaques were randomly divided into 4 groups. Group 1 ($n = 1$) received vehicle (1:1:18 of emulphor:alcohol:

TABLE 1 Animal IDs, duration of infection, SIV inoculum, and plasma and intestinal viral loads in VEH/SIV and THC/SIV macaques[a]

Inoculum group and animal ID	Plasma viral loads (10^6 copies/ml) at day p.i.:			Intestinal viral loads (10^6 copies/mg RNA) at day 60 p.i.	Intestinal histopathology at necropsy
	14	30	60		
THC only					
HM74	NA	NA	NA	NA	ND
GP68	NA	NA	NA	NA	ND
HE44	NA	NA	NA	NA	ND
VEH/SIV					
FE07	10	2.7	3.5	0.07	ND
HH45	12	1	0.3	0.04	ND
HT49	8	0.1	0.4	0.1	Severe lymphoid hyperplasia
HN54	24	1.3	0.8	20	Mild colitis
THC/SIV					
FT59	2.7	0.05	0.02	0.06	Mild typhlitis with nematodes
GP68	16	5.1	22	6	ND
HN56	6.6	0.06	0.3	0.2	ND
HV47	34	1	2	2	ND
VEH only (control)					
IC52	NA	NA	NA	NA	ND

[a] Animals were divided into two cohorts (cohort 1: HE44, GH61, FE07, HH45, FT59, GP68; cohort 2: IC52, HM74, HT49, HN54, HN56, HV47). NA, not applicable; ND, none detected.

saline) and no infection. Group 2 ($n = 3$) received twice-daily intramuscular injections of Δ^9-THC and no infection. Group 3 ($n = 4$) received twice-daily injections of vehicle (VEH) and were infected intravenously with 100 50% tissue culture infective doses ($TCID_{50}$) of SIVmac251. Group 4 ($n = 4$) received twice-daily injections of Δ^9-THC similar to group 2 for 4 weeks prior to SIV infection. The animals were studied in two cohorts (cohort 1 consisted of animals identified as HE44, GH61, FE07, HH45, FT59, and GP68; cohort 2 consisted of IC52, HM74, HT49, HN54, HN56, and HV47) (Table 1). Chronic administration of Δ^9-THC (or 0.05 ml/kg of body weight VEH) was initiated 4 weeks before SIV infection at 0.18 mg/kg. This dose of THC was found to eliminate responding in a complex operant behavioral task in almost all animals (10). After 2 weeks, the dose was increased to 0.32 mg/kg, and this dose was continued for the entire duration of the study. Proximal duodenal pinch biopsy specimens were collected once before SIV inoculation and at 14 and 30 days postinfection (days p.i.). Intestinal pinch biopsies were performed by laboratory animal veterinarians. Animals were preanesthetized with ketamine hydrochloride, acepromazine, and glycopyrolate, intubated, and maintained on a mixture of isoflurane and oxygen. All animals were necropsied at 60 days p.i. Pinch biopsy specimens and tissue samples collected at necropsy were stored in RNAlater (Ambion, TX). Duodenal tissue from all animals was collected immediately and fixed in 10% neutral buffered formalin for histopathologic evaluation.

SIV levels in plasma were quantified by a real-time qRT-PCR assay that targets the *gag* gene as previously described (23). Similarly, SIV RNA levels in duodenal tissue were quantified in tissues preserved in RNAlater (Life Technologies) as described before (37) and normalized to milligrams of total RNA.

Flow cytometry to quantify intestinal $CD4^+$ T cell dynamics. Intestinal lamina propria leukocytes (LPLs) were isolated and adjusted to a concentration of 10^7/ml. For T cell immunophenotyping, ~100-μl aliquots were stained with appropriately diluted, directly conjugated monoclonal antibodies to CD3 (Alexa Fluor 700:SP34-2; BD Biosciences, San Jose, CA), CD4 (eFluor 450:OKT4; eBioscience, Inc., CA, USA), and CD8 (AmCyan: SK1; BD Biosciences). Samples were stained for 30 min in the dark at 4°C, fixed in 2% paraformaldehyde, and stored in the dark at 4°C overnight for acquisition the next day. Samples were acquired on LSR II flow cytometry equipment (BD Biosciences) and analyzed with FlowJo software (Treestar Inc., Ashland, OR). The cells were first gated on singlets followed by lymphocytes and $CD3^+$ T cells and then on $CD3^+CD4^+CD8^{+/-}$ and $CD3^+$ $CD4^{+/-}$ $CD8^+$ T cell subsets. All flow cytometric analysis was performed by the LSUHSC Comprehensive Alcohol Research Center Core Laboratory.

Global microRNA profiling using TaqMan OpenArray platform. Total RNA from pinch biopsy specimens and intact duodenal tissue samples was isolated using the miRNeasy total RNA isolation kit (Qiagen Inc., CA) according to the manufacturer's protocol. Approximately 100 ng total RNA was first reverse transcribed using the microRNA reverse transcription (RT) reaction kit (Life Technologies, Grand Island, NY).

Briefly, two master mixes representing either open-array panel (panel A and panel B) were prepared for each RNA sample, which consisted of the following reaction components: 0.75 μl MegaPlex RT primers (10×), 0.15 μl deoxynucleoside triphosphates (dNTPs) with dTTP (100 mM), 1.50 μl MultiScribe reverse transcriptase (50 U/μl), 0.75 μl 10× RT buffer, 0.90 μl $MgCl_2$ (25 mM), 0.09 μl RNase inhibitor, and 0.35 μl nuclease-free water (20 U/μl). Three microliters of total RNA (100 ng) was loaded into the appropriate wells of a 96-well plate, and 4.5 μl of the RT reaction master mix was added into the appropriate well. After a brief spin and 5 min of incubation on ice, samples in the 96-well plate were subjected to the following thermal cycling conditions on the ABI 7900 HT Fast PCR system: standard or maximum ramp speed, 16°C for 2 min, 42°C for 1 min, 50°C for 1 s (40 cycles), 85°C for 5 min (hold), 23°C (hold). Immediately after thermal cycling, the 96-well plate containing cDNA was stored at −80°C.

For the preamplification, 2.5 μl of the cDNA from each sample was mixed with a total of 22.5 μl of preamplification reaction master mix, consisting of 12.5 μl TaqMan PreAmp master mix (2×), 2.5 μl Megaplex PreAmp primers (10×), and 7.5 μl nuclease-free water in a 96-well plate. After a brief vortex and spin, samples in the 96-well plate were subjected to the following thermal cycling conditions on the ABI 7900 HT Fast PCR system: standard or maximum ramp speed, hold at 95°C for 10 min, hold at 55°C for 2 min, hold at 72°C for 2 min, 12 cycles at 95°C for 15 s and at 60°C for 4 min, hold at 4°C. The preamplified product was diluted 40 times by mixing 4 μl of the preamplified product with 156 μl of 0.1× Tris-EDTA (TE), pH 8.0, and loaded onto TaqMan OpenArray human

microRNA plates for processing using the QuanStudio 12K flex Real Time PCR system (Life Technologies).

Quantitative real-time TaqMan and SYBR green RT-PCR assay for OpenArray validation. To validate OpenArray data and at the same time ascertain that the differentially expressed miRNAs were not the result of false discovery, the relative expressions of six differentially expressed miRNAs (miR-10a, miR-24, miR-99b, miR-145, miR-149, and miR-187) were further determined by individual TaqMan miRNA assays. Approximately 200 to 250 ng of total RNA was reverse transcribed using the stem-loop primers provided in the predesigned kit, and ~4 μl of cDNA was subjected to 40 cycles of PCR on the ABI 7900 HT Fast PCR system (Life Technologies) using the following thermal cycling conditions: 95°C for 10 min followed by 40 repetitive cycles of 95°C for 15 s and 60°C for 1 min. As a normalization control for RNA loading, RNU48 and snoU6 were amplified in duplicate wells on the same multiwell plate. Proinflammatory cytokine gene expression in duodenum samples was determined by the Power SYBR green RNA-to-C_T 1-Step RT-PCR assay (Life Tech). Each quantitative real-time (qRT)-PCR mixture (20 μl) contained the following: 2× Power SYBR green master mix (12.5 μl), forward and reverse primers; for tumor necrosis factor alpha (TNF-α), forward primer (For), 5′-TACCAGACCAAGGTCAACCTCCTC-3′, and reverse (Rev), 5′-GCTGAGTCGATCACCCTTCTCCA-3′); for interleukin-1β (IL-1β) For, 5′-TGGCATCCAGCTACAAATCTCCCA-3′, and Rev, 5′-AAGGGAATCAAGGTGCTCAGGTCA-3′); for MCP-1, For, 5′-TAGGAAGATCTCAGTGCAGAGGCT-3′, and Rev, 5′-GTCCATGGAATCCTGAACCCACTT-3′); for CXCL11, For, 5′-ATGAGTGTGAAGGGCATGGCTA-3′, and Rev, 5′-GAACATAGGGAAACCTTGAACAACCGTA-3′); for gamma interferon (IFN-γ), For, 5′-CGGTAACTGACTTGAATGTCCAACGC-3′, and Rev, 5′-GGACAACCATTACTGGGATGCTCTTC-3′); for GAPDH (glyceraldehyde-3-phosphate dehydrogenase), For, 5′-CAAGAGAGGCATTCTCACCCTGAA-3′, and Rev, 5′-TGGTGCCAGATCTTCTCCATGTC-3′); for 18s rRNA, For, 5′-GCTACCACATCCAAGGAAGGCA-3′, and Rev, 5′-AGGGCCTCGAAAGAGTCCTGTATT-3′); and for beta-actin, For, 5′-CAACAGCCTCAAGATCGTCAGCAA-3′, and Rev, 5′-GAGTCCTTCCACGATACCAAAGTTGTC-3′] (200 nM), and 200 ng of total RNA. Comparative real-time PCR was performed in duplicate wells including no template controls, and relative change in gene expression was calculated using the comparative threshold cycle ($\Delta\Delta C_T$) method.

***In situ* hybridization and immunofluorescence for cellular localization of miR-99b and NOX4.** *In situ* hybridization for miR-99b was performed using locked nucleic acid (LNA)-modified DNA probes (Exiqon Inc., Denmark). Briefly, 7-μm-thick formalin-fixed, paraffin-embedded tissue sections were first deparaffinized, rehydrated in a descending series of ethanol, and pretreated in a microwave with citrate buffer (antigen unmasking solution; Vector Laboratories, Burlingame, CA) for 20 min at high power according to the manufacturer's instructions. Thereafter, sections were thoroughly washed, placed in a humidified chamber, and prehybridized at 45°C with 1× microRNA *in situ* hybridization buffer (Exiqon Inc., Denmark). A digoxigenin-labeled LNA-modified miR-99b DNA probe (5FamN/AACCCAATATCAAACATATCA/3_N/) or scrambled probe (5FamN/GTGTAACACGTCTATACGCCCA/3_N/) was used at a 40 nM concentration in hybridization buffer and hybridized overnight at 50°C. Exiqon recommends using a hybridization temperature at least 30°C less than the RNA melting temperature (T_m) of the probe (87°C for miR-99b and 87°C for scrambled). After hybridization, slides were washed with 5× SSC (standard saline citrate buffer; 1× SSC is 0.15 M NaCl plus 0.015 M sodium citrate), 2× SSC, and 0.1× SSC and blocked with Dako protein-free blocker (Dako Laboratories) for 1 h. Fab fragments of an antidigoxigenin antibody conjugated with alkaline phosphatase (Roche Diagnostics Corporation, Penzberg, Germany) were used to detect digoxigenin-labeled probes. Positive signals were detected using permanent red substrate according to the manufacturer's (Dako Laboratories) instructions. Controls included matched tissues hybridized with LNA-modified scrambled probes.

TABLE 2 Schematic representation of NOX4 3′ UTR depicting predicted binding site for miR-99b[a]

Strand	Target site sequence
NOX4 mRNA	5′–AAGACUCUGUAUUGAU**ACGGGU**A
miR-99b	3′–GCGUUCCAGCCAAGA**UGCCCA**C

[a] GenBank accession number for NOX4 mRNA, NM_001143836; binding sites on 3′ UTR were positions 515 to 522. The NOX4 mRNA site is conserved in humans, chimpanzee, macaque, orangutan, and mouse. The prediction algorithm used was TargetScan (38). Boldface nucleotides show seed region (2-7) of miR-99b and its complementary bases on the 3′ UTR of NOX4 mRNA.

Immunofluorescence for detecting CXCL12 (rabbit anti-mouse/Rat CXCL12 alpha; 1 in 200 dilution; eBiosciences), rabbit anti-human SDF1 (rabbit anti-rat polyclonal antibody; 1 in 100 dilution; LifeSpan Biosciences), and NOX4 (rabbit anti-human polyclonal antibody; 1 in 100 dilution; LifeSpan Biosciences) was done as previously described (17, 23).

Cloning of 3′-UTR of NOX4 mRNA and Dual-Glo luciferase reporter gene assay. The 3′ untranslated region (UTR) of the rhesus macaque NOX4 mRNA contains a single predicted miR-99b binding site (TargetScan 6.2) (38) (Table 2). Accordingly, a short 52-nucleotide sequence representing the 3′ UTR containing the predicted miR-99b site (5′-GATGTTTGAAAACACAGCACAAGACTCTGTATTGA*TACGGGT*ACTTTGTGTC-3′) (where the predicted binding site is in italics) was synthesized (IDTDNA Technologies Inc., IA) for cloning into the pmirGLO Dual Luciferase vector (Promega Corp., Madison, WI). A second oligonucleotide with the miRNA binding site (8 nucleotides) deleted (5′-GATGTTTGAAAACACAGCACAAGACTCTGTATTGACTTTGTGTC-3′) was also synthesized to serve as a negative control. The oligonucleotide sequence was synthesized with a Pme1 site on the 5′ end and an XbaI site on the 3′ end for directional cloning. The pmirGLO vector was first cut with Pme1 and XbaI restriction enzymes, gel purified, and ligated with either wild-type sequence containing the miR-99b binding site (NOX4-wtUTR) or deleted sequence (NOX4-delUTR). HEK293 cells were plated at a density of 2×10^4 cells per well of a 96-well plate. At 60 to 70% confluence, cells were cotransfected with ~100 ng NOX4-wtUTR or NOX4-delUTR luciferase reporter vector and 100 nM miR-99b mimic using the Dharmafect Duo transfection reagent (ThermoFisher Scientific). In separate wells, cells were also transfected with pmirGLO vector (Promega Corp) as a normalization control. After 72 h, the Dual Glo luciferase assay was performed according to the manufacturer's recommended protocol using the BioTek H4 Synergy plate reader (BioTek, Winooski, VT). The normalized firefly-to-renilla ratio was calculated to determine the relative reporter activity. Experiments were performed in 6 replicates and repeated three times.

Quantitative image analysis. Quantitation of cells and regions of interest (ROI) labeled by LNA-modified miR-99b *in situ* hybridization probes was performed using Volocity 5.5 software (PerkinElmer Inc., MA, USA) after capturing images on a Leica confocal microscope. Several ROI were hand drawn on the epithelial and lamina propria regions in the images from duodenum. The data were first graphed and then analyzed using the Mann-Whitney U test (Wilcoxon's rank sum test) employing the Prism v5 software (GraphPad software). P values of <0.05 were considered statistically significant.

ELISA for quantifying plasma LBP levels. Lipopolysaccharide (LPS) binding protein (LBP) levels in plasma in all macaques at necropsy were quantified using a commercially available enzyme-linked immunosorbent assay (ELISA; Biometec, Greifswald, Germany) according to the manufacturer's recommended protocol. Samples were assayed in duplicate.

Data analysis and data availability. QuantStudio run files from all groups were analyzed simultaneously using ExpressionSuite software v1.0.2 (Life Technologies). ExpressionSuite Software utilizes the comparative threshold cycle ($\Delta\Delta C_T$) method to rapidly and accurately quantify relative gene expression across a large number of genes and samples. The software provides the option to normalize gene expression data using

either endogenous controls or global normalization and provides fold changes with *P* values. miRNA expression data were normalized to all three endogenous controls (RNU44, RNU48, and snoU6). In all experiments, the C_T upper limit was set to 28, meaning that all miRNA detectors with a C_T value greater than or equal to 28 were excluded. A *P* value of ≤0.05 was considered significant. Because this is an exploratory study with a small sample size, we did not apply multiple-comparisons correction (Benjamini-Hochberg method for false-discovery rate) mainly to avoid type II error (false negatives). However, to avoid type I error (false positives), we confirmed the expression of at least six miRNAs using qRT-PCR.

For individual miRNA qRT-PCR confirmation studies (miR-10a, miR-24, miR-99b, miR-45, miR-149, and miR-187), the VEH/SIV macaque with the highest ΔC_T value served as the calibrator/reference and was assigned a value of 1. All differentially expressed miRNAs in the THC/SIV and VEH/SIV groups are shown as an *n*-fold difference relative to this macaque. This approach was taken mainly to facilitate graphing the control (VEH/SIV) samples so that the variation within the control samples could be displayed. Individual miRNA qRT-PCR data were analyzed using nonparametric Wilcoxon's rank sum test for independent samples using the RealTime Statminer package, a bioinformatics software developed by Integromics on Spotfire DecisionSite. Differences in the total number of $NOX4^+$ duodenal crypt epithelial cells between VEH/SIV and THC/SIV macaques were analyzed using the Mann Whitney U test employing the Prism v5 software (GraphPad software). Firefly/renilla ratios were statistically analyzed using an unpaired *t* test.

Microarray data accession number. TaqMan OpenArray microRNA data files were deposited in the GEO database under accession number GSE61654 (http://www.ncbi.nlm.nih.gov/geo/query/acc.cgi?acc=GSE61654).

RESULTS

Plasma and intestinal viral loads, CD4 and CD8 T cell status and intestinal histopathology. All VEH/SIV ($n = 4$) and THC/SIV ($n = 4$) macaques inoculated intravenously with 100 $TCID_{50}$ of SIVmac251 had detectable plasma and tissue (duodenum) viral loads at 14, 30, and 60 days p.i. (Table 1). Intestinal $CD4^+$ T cell data were available only for cohort 2. As shown in Fig. S1A in the supplemental material, $CD4^+$ T cells were markedly depleted in both VEH/SIV (HN54 and HT49) and THC/SIV (HN56 and HV47) groups compared to the animal that received only VEH (IC52) or THC (HM74) at 14 and 30 days p.i. Interestingly, $CD4^+$ T cell percentages were higher in both animals at 60 days p.i. in the THC/SIV group than in the VEH/SIV group, suggesting possible signs of $CD4^+$ T cell recovery (see Fig. S1A in the supplemental material). Further, $CD4^+$ T cell percentage in one of the THC/SIV macaques (HV47) at the 60 days p.i. time point was no different from that in the uninfected macaque (HM74) that received only THC. No major differences in $CD8^+$ T cells percentages were noticed between the two groups (see Fig. S1B in the supplemental material). Histopathological analysis revealed the presence of severe lymphoid hyperplasia and mild colitis in two of the four VEH/SIV macaques. Only one of the four macaques in the THC/SIV group had detectable intestinal lesions mainly due to nematode infestation (mild typhlitis with nematodiasis) (Table 1).

THC administration to uninfected and SIV-infected macaques caused marked alterations in intestinal miRNA expression. In order to determine if the protective effect of Δ^9-THC administration in SIV-infected macaques was associated with alterations in miRNA expression, we performed global miRNA profiling of duodenal tissue during acute SIV infection using the TaqMan OpenArray human microRNA plates (Life Technologies). The baseline/preinfection biopsy samples collected from all 12 animals were used as a reference control to identify differentially expressed miRNAs in the three target groups, namely, THC only ($n = 3$), VEH/SIV ($n = 4$), and THC/SIV ($n = 4$) at 14, 30, and 60 days p.i. (Table 1). In addition, all three animals in the THC-only group had pinch biopsy specimens collected at the same time points as in the VEH/SIV and THC/SIV groups to determine the effect of THC administration alone on intestinal miRNA expression. As shown in Table 3, the total number of differentially expressed miRNAs steadily increased in the VEH/SIV and THC/SIV groups from 14 days p.i. to 60 days p.i. At 14 days p.i., a larger number of miRNAs showed decreased expression in both groups (Table 3). At 30 days p.i., the numbers of miRNAs showing increased or decreased expression were almost equal in the two groups (Table 3). The QuantStudio run file representing one THC/SIV macaque (FT59) at the 30 days p.i. time point did not pass quality control (QC) and was not included in the analysis. However, at 60 days p.i., ~28% (13/47) of the differentially expressed miRNAs were downregulated in the VEH/SIV group compared to the THC/SIV group, where none of the differentially expressed miRNAs showed reduced expression (Table 3). In contrast, all 59 differentially expressed miRNAs were upregulated in the THC/SIV group at 60 days p.i. (Table 3). Similarly, the total number of differentially expressed miRNAs in the THC uninfected group increased as the duration of THC treatment increased from 14 days to 60 days (Table 3). Interestingly, in this group, almost 80 to 90% of the differentially expressed miRNAs at all three time points predominantly showed increased expression (Table 3). The miRNA IDs, raw C_T, fold changes, and *P* values of all differentially expressed miRNAs at each time point in the three different groups are shown separately in supplemental Tables S1 to S3 in the supplemental material. We decided to present the raw C_T values mainly because they provide valuable information on the relative abundance of each miRNA species in the intestine. Overall, these findings suggest that chronic THC administration positively modulates miRNA expression in the intestine. Given that T cell ($CD8^+$ and $CD4^+$) activation is accompanied by marked downregulation of miRNA expression (39–42), the notable absence of downregulation in THC/SIV macaques at 60 days p.i. suggests that THC may provide protection by preventing immune cell activation.

TABLE 3 Total number of miRNAs that showed statistically significant differential expression ($P < 0.05$) in THC-only, VEH/SIV, and THC/SIV groups at 14, 30, and 60 days p.i. with reference to the preinfection time point

Biological group, time point	No. of miRNAs		
	Differentially expressed (total)	Upregulated	Downregulated
THC only, 14 days	7	6	1
THC only, 30 days	29	26	3
THC only, 60 days	44	35	9
VEH/SIV, 14 days p.i.	23	7	16
VEH/SIV, 30 days p.i.	26	11	15
VEH/SIV, 60 days p.i.	47	34	13
THC/SIV, 14 days p.i.	17	3	14
THC/SIV, 30 days p.i.	31	15	16
THC/SIV, 60 days p.i.	59	59	0

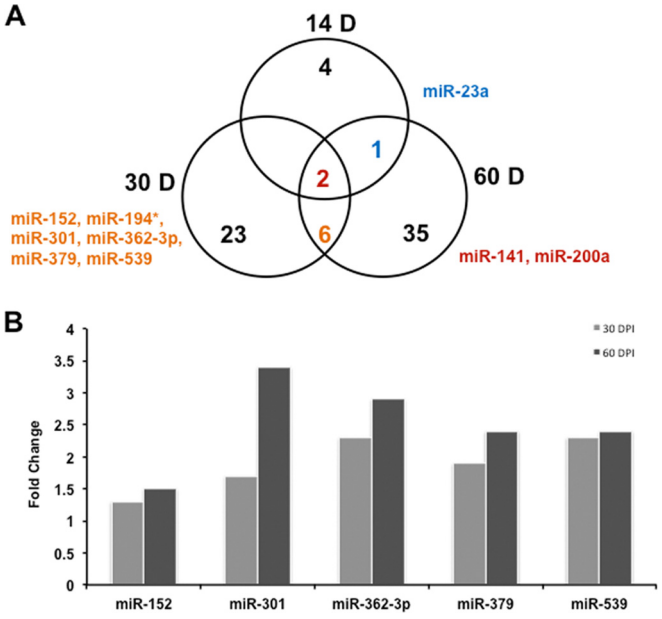

FIG 1 The differential expression of miRNAs in the duodenum of uninfected animals at all time points (14, 30, and 60 days [D] posttreatment) after chronic THC administration. (A) The Venn diagram shows miRNAs whose expression overlapped between time points and common to all time points. (B) THC produced dose- and time-dependent increases in the expression of about five miRNAs in the duodenum of uninfected animals.

THC administration to uninfected macaques caused selective upregulation of miR-141 and miR-200a expression in the duodenum at all three time points. THC administration induced the differential expression of 7 miRNAs at 14 days, 29 miRNAs at 30 days, and 44 miRNAs at 60 days in uninfected animals (Table 3). To identify an miRNA signature specific to chronic THC treatment, we used a Venn diagram to categorize the differentially expressed miRNAs at the three different time points. When comparing all three time points to each other, the expressions of nine miRNAs were found to overlap and two miRNAs, miR-141 and miR-200a, were found to be commonly upregulated at all three time points (Fig. 1A). The two miRNAs share a similar seed sequence and accordingly have identical predicted targets (TargetScan 6.2) (38). miR-141 was recently shown to be downregulated in the colon of trinitrobenzenesulfonic acid (TNBS)-induced colitis in mice, which led to elevated expression of CXCL12β, a predicted target of miR-141 (43). Interestingly, with the exception of miR-194*, all miRNAs whose expression overlapped between time points (miR-152, miR-301, miR-362-3p, miR-379, and miR-539 between 30 and 60 days and miR-23a between 14 and 60 days), including miR-141 and miR-200a (which overlapped at all three time points), have bioinformatically predicted binding sites on the 3′ UTR of human and rhesus macaque CXCL12 mRNA (TargetScan 6.2) (38) (see Tables S4 to S7 in the supplemental material). Moreover, potential binding sites for all of the above THC-induced miRNAs have also been predicted by the miRanda algorithm (44). In addition, the expression of five of six miRNAs that overlapped between the 30- and 60-day time points showed a time-dependent increase in expression (Fig. 1B), demonstrating that THC treatment alone positively modulated the expression of miRNAs with potential anti-inflammatory effects in the intestine.

We next performed immunofluorescence studies using two anti-CXCL12 antibodies, but neither cross-reacted with the rhesus macaque, and as a result it remains unclear if increased expression of CXCL12-targeting miRNAs is accompanied by a concomitant decrease in CXCL12 protein expression in the intestine. Put together, these novel and interesting results suggest that chronic THC administration induces the expression of a select cluster of miRNAs that may exert anti-inflammatory effects in the intestine by directly targeting CXCL12 expression, a chemokine well known to regulate the trafficking of T cells and macrophages into the intestinal lamina propria, causing progression of GI inflammation (45, 46).

THC and SIV exert synergistic and additive effects on intestinal expression of miR-29b, miR-101, miR-130a, miR-218, and miR-374 at 60 days p.i. We again used a Venn diagram to study the relationship between the differentially expressed miRNAs at all three time points in the THC-only, VEH/SIV, and THC/SIV groups. At 14 days p.i., the expression of five miRNAs overlapped between the VEH/SIV and THC/SIV groups. However, the expression of only one miRNA in the THC uninfected group overlapped with the VEH/SIV or THC/SIV group (Fig. 2A). Consistent with our recent finding (37), miR-190b was significantly upregulated in the intestine in response to SIV infection in both VEH and THC groups. However, as shown in Tables S2 and S3 in the supplemental material, miR-190b fold change was higher in the VEH/SIV group (~6.5-fold) than in the THC/SIV group (~4.6-fold), suggesting that the protective effects of THC at this time point may be partially mediated by the reduction in the magnitude of miR-190b expression.

At 30 days p.i., the expression of 11 miRNAs overlapped among all groups, and one was common to all three groups (Fig. 2B). The expression of two miRNAs overlapped between the THC-only and the VEH/SIV groups at 30 days p.i. (Fig. 2B). Further, while the expression of both CXCL12-targeting miRNAs (miR-200a and miR-362-3p) was elevated in both groups, the fold change was slightly higher in the THC-only group (1.9- and 2.3-fold) than in the VEH/SIV group (1.5- and 1.4-fold) (see Tables S1 and S2 in the supplemental material). miR-150 is an important miRNA that is rapidly and efficiently downregulated during immune cell activation (39–41). In agreement with the above findings (39–41), miR-150 showed significantly reduced expression (1.9-fold decrease) only in the VEH/SIV group (see Table S2 in the supplemental material). Reduced miR-150 expression may indirectly suggest early immune cell activation in the intestinal lamina propria of the VEH/SIV compared to the THC/SIV group. At this time point, miR-301, also predicted to directly target CXCL12, showed almost identical expression levels (~1.7-fold increase) in the THC-only and THC/SIV groups (see Tables S1 and S3 in the supplemental material).

At 60 days p.i., 29 miRNAs overlapped among all three groups and the expression of seven miRNAs was common to all three groups (Fig. 2C). Interestingly, from the results shown in Fig. 2D it is evident that THC exerted synergistic and additive effects on the expression of six of seven miRNAs, which included miR-29b, miR-101, miR-106b, miR-130a, miR-218, and miR-374. The fold change in the expression of miR-362-3p was more or less similar in all three groups (~2.7- to 2.9-fold). Further, among the seven, miR-29b, miR-101, miR-130a, and miR-362-3p have bioinformatically predicted binding sites on the 3′ UTR of CXCL12 (see Tables S5 and S7 in the supplemental material). Similarly, miR-

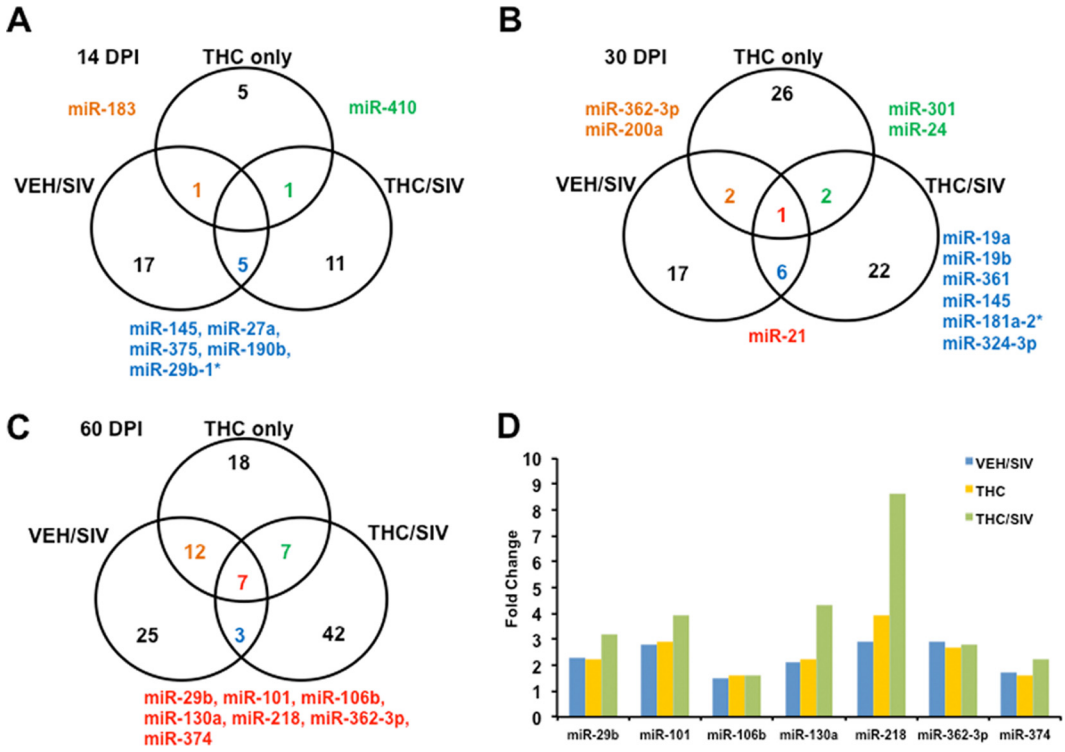

FIG 2 Synergistic and additive effects exerted by THC and SIV on the expression of select miRNAs in the duodenum. Comparison of miRNA expression at 14 (A), 30 (B), and 60 (C) days following SIV infection (DPI) in the three treatment groups (THC only, VEH/SIV, and THC/SIV) using a Venn diagram. (D) THC and SIV exerted additive and synergistic effects on the expression of miR-29b, miR-101, miR-106b, miR-130a, miR-218, and miR-374 at 60 days p.i.

218, an miRNA previously shown to exert anti-inflammatory effects by directly targeting Robo1 protein translation (47), showed markedly elevated expression in the THC/SIV group (8.6-fold increase) compared to the VEH/SIV (3.9-fold increase) and THC-only (2.9-fold increase) groups (see Tables S1 to S3 in the supplemental material). Similar to the 30-day p.i. time point, miR-150 showed statistically significant decrease in expression only in the VEH/SIV group, suggesting persistent immune cell activation (39–41). Overall, these results suggest that the elevated intestinal expression of miR-29b, miR-101, miR-106b, miR-130a, miR-218, miR-362-3p, and miR-374 is likely to be a part of the normal anti-inflammatory response exerted by the host to SIV infection. However, chronic administration of THC to SIV-infected macaques may strengthen this response by exerting additive and synergistic effects on the intestinal expression of these anti-inflammatory miRNAs.

THC specifically upregulates a cluster of six anti-inflammatory miRNAs in the duodenum compared to VEH-administered SIV-infected macaques at 60 days p.i. To specifically identify miRNAs induced by THC in SIV-infected macaques, we performed the same analysis as the one described earlier, but this time we used the VEH/SIV group as a reference and made comparisons relative to the THC/SIV group at 14, 30, and 60 days p.i. Based on the analysis, 3 and 6 miRNAs showed differential expression in the THC/SIV group at 14 days p.i. and 30 days p.i., respectively (Table 4; see also Table S8 in the supplemental material). In contrast, about 19 miRNAs were found to be differentially expressed in the THC/SIV group at 60 days p.i. (Table 4; see also Table S8 in the supplemental material). Interestingly, all 19 miRNAs showed significantly elevated expression in the THC/SIV group compared to the VEH/SIV group (Table 4; see also Table S8 in the supplemental material). Among the these, miR-10a, miR-24, miR-99b, miR-145, miR-149, and miR-187 have been previously reported to regulate inflammation (48–54). As shown in Fig. 3A to F, miR-24, miR-149, and miR-99b showed statistically significant elevation in the THC/SIV group when analyzed using nonparametric Wilcoxon's rank sum test. The differences in expression of the remaining 3 miRNAs, namely, miR-10a ($P = 0.06$), miR-187 ($P = 0.06$), and miR-145 ($P = 0.11$), did not reach statistical significance (Fig. 3A, D, and F). The raw C_T, ΔC_T, $\Delta\Delta C_T$, and fold changes for all 6 miRNAs in VEH/SIV and THC/SIV macaques are shown in Table S9 in the supplemental material. To further explore the functional relevance of the changes in miRNA expression seen in the THC/SIV animals, we also quantified mRNA expression of TNF-α, IL-1β, MCP-1, CXCL11, and IFN-γ in duodenum samples collected at necropsy. Contrary to our prediction, no significant differences in inflammatory cytokine gene expression were detected be-

TABLE 4 Number of miRNAs that showed statistically significant differential expression in THC/SIV macaques at the three different time points compared to VEH/SIV macaques

Biological group, no. of days p.i.	No. of miRNAs		
	Differentially expressed (total)	Upregulated	Downregulated
THC/SIV, 14	3	2	1
THC/SIV, 30	6	2	4
THC/SIV, 60	19	19	0

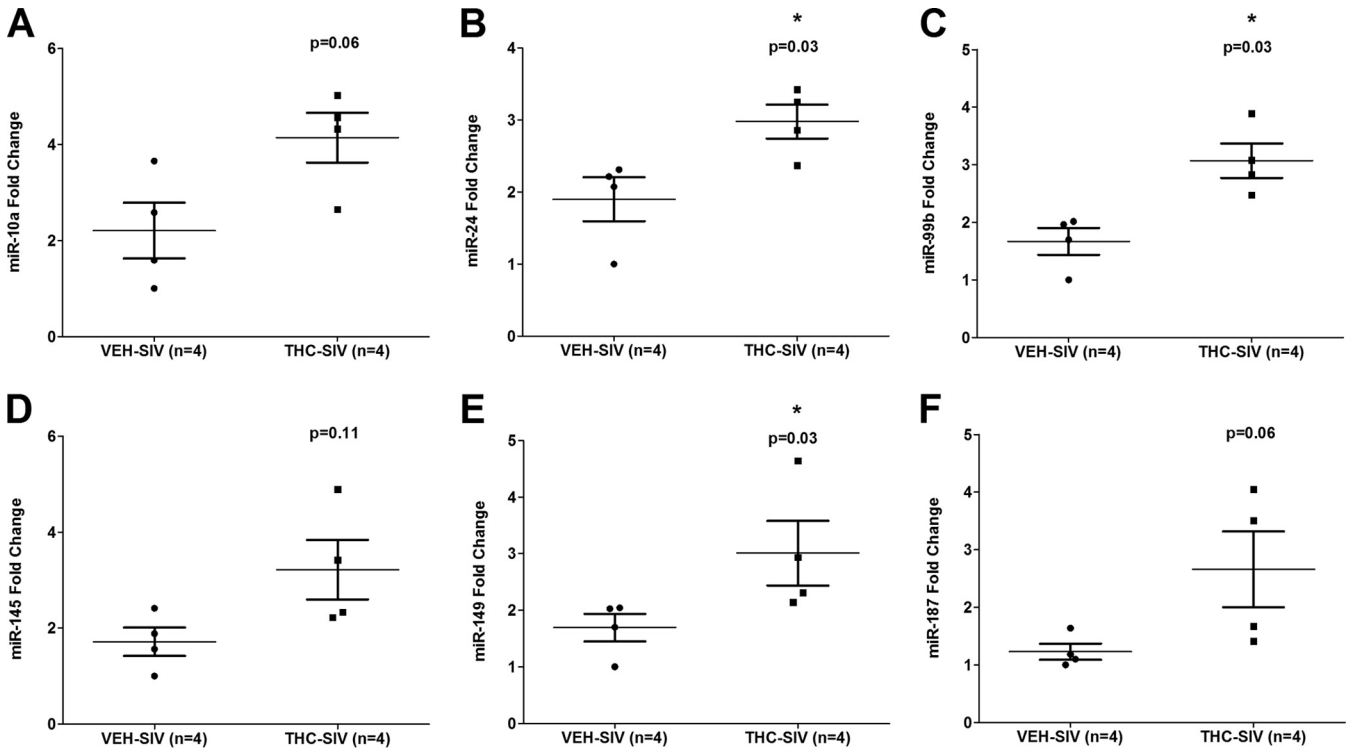

FIG 3 Significant elevation of miR-24 (B), miR-99b (C), and miR-149 (E) expression in the duodenum of THC/SIV macaques compared to VEH/SIV macaques at 60 days p.i. miR-10a (A), miR-145 (D), and miR-187 (F) did not show statistical significance ($P = 0.06$ to 0.11). Data were analyzed using the nonparametric Wilcoxon's rank sum test method. The error bars represent standard errors of mean fold changes within each group. A single asterisk indicates statistical significance ($P < 0.05$).

tween the THC/SIV and VEH/SIV macaques (see Fig. S2 in the supplemental material). Collectively, these findings suggest that an important epigenetic mechanism underlying the anti-inflammatory effects of THC in the intestine of SIV-infected macaques involves the selective upregulation of anti-inflammatory miRNA expression.

NOX4 is a direct target of miR-99b, and its protein expression is significantly increased in the intestinal epithelium of VEH/SIV compared to THC/SIV-infected macaques at 60 days p.i. Because miR-99b showed statistically significant elevation in the THC/SIV group and it has also been previously shown to influence the fate of intestinal epithelial cells (55), we decided to further investigate its expression and possible function in the intestine. Inhibition of miR-99b in dendritic cells using antagomirs has been reported to markedly increase the production of IL-6, IL-12, and IL-1β, clearly highlighting its anti-inflammatory properties (52). Accordingly, we first performed *in situ* hybridization to identify the mucosal compartment (epithelium versus lamina propria cells) in the intestine expressing miR-99b. As shown in Fig. 4A and B (for VEH/SIV) and Fig. 4D and E (for THC/SIV), miR-99b localized to the duodenal epithelial and lamina propria cells. Overall, the intensity of miR-99b staining was stronger in the two THC/SIV macaques (Fig. 4D and E) than in the VEH/SIV macaques (Fig. 4A and B). Moreover, miR-99b staining in the duodenum of one VEH/SIV macaque (HT49 [Fig. 4B]) was considerably weaker than the staining in both THC/SIV macaques. Images from all 4 macaques were captured using the same laser (red and green) strength and processed using Volocity 5.5 software (PerkinElmer Inc., MA, USA) utilizing the same brightness, density, and black level settings. Image analysis confirmed significantly ($P < 0.05$) elevated miR-99b *in situ* staining intensity in the duodenum of THC/SIV macaques compared to the VEH/SIV macaques (Fig. 4F). The observed difference in miR-99b staining intensity between the two groups agrees well with the qRT-PCR raw C_T data shown in Table S9 in the supplemental material (tab 3). Consistent with the *in situ* hybridization data, both miR-99b raw C_T and dC_T (ΔC_T) values are larger in the two VEH/SIV macaques (FE07 and HT49) than in the THC/SIV macaques (HN56 and HV47) (see Table S9, tab 3, in the supplemental material). Additionally, *in situ* miR-99b signal intensity in the duodenum of uninfected control macaques was even weaker (see Fig. S3 in the supplemental material) and is consistent with the qRT-PCR data showing an ~3.9-fold increase in THC/SIV macaques compared to preinfection controls (see Table S3, tab 3, in the supplemental material).

To better understand the biological significance of miR-99b upregulation in the THC/SIV group, we next focused on NOX4 expression, a predicted target of miR-99b for a couple of reasons. First, the activity of NOX4, a potent reactive oxygen species (ROS)-generating enzyme was shown to be significantly attenuated by the CB2 agonist HU-308 in the kidneys of cisplatin-treated rats (7). Second, and more importantly, inhibition of NADPH oxidase activity in colonic epithelial cells isolated from ulcerative colitis patients increased cell viability and considerably decreased ROS and TNF-α levels following LPS treatment (56). Therefore, we performed immunofluorescence studies using a polyclonal NOX4 antibody to identify the cell types in the intestine expressing NOX4. Interestingly, increased numbers of $NOX4^+$ crypt epithelial cells were very conspicuous in the intestinal mucosa of both VEH/SIV-treated macaques (Fig. 4A and B). Further, NOX4 localized to the cytoplasm of crypt epithelial cells (Fig. 4C). In contrast, occasional $NOX4^+$ epithelial cells were detected in the du-

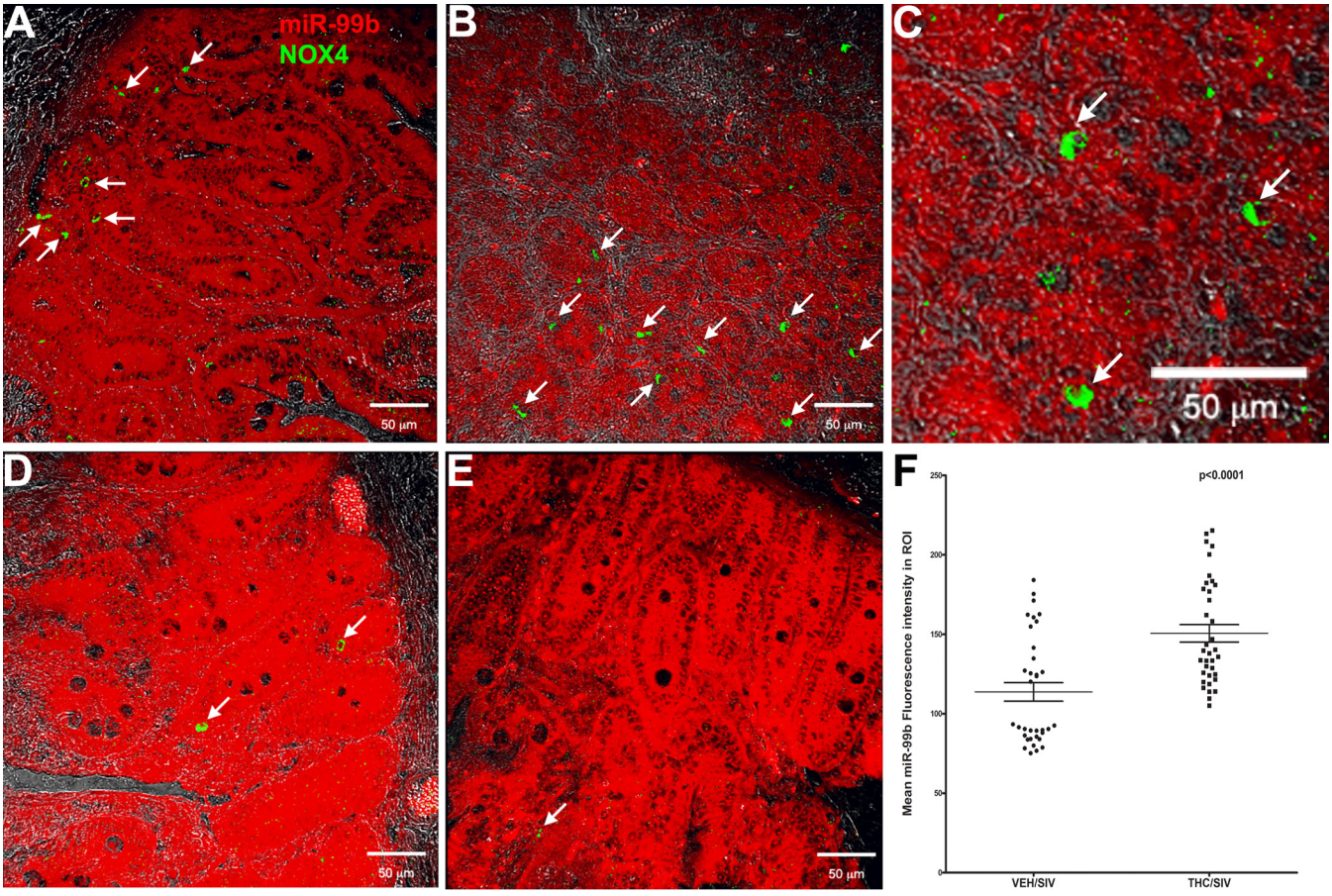

FIG 4 Localization of miR-99b to both duodenal epithelium and lamina propria cells (A, B, D, and E) in both VEH/SIV (FE07, HT49) and THC/SIV (HN56, HV47) macaques. Note the increased miR-99b staining intensity in the THC/SIV macaques (D and E) compared to the VEH/SIV macaques (A and B). Increased numbers of duodenal crypt epithelial cells from both VEH/SIV macaques stained positive for NOX4 (A and B). (C) A close-up view of the lower right quadrant of panel B clearly shows NOX4 staining localized to the epithelial cell cytoplasm. In contrast, duodenal crypt epithelial cells from both THC/SIV macaques (D and E) show occasional NOX4$^+$ cells. Small white arrows (A, B, D, and E) point to NOX4$^+$ crypt epithelial cells. Epithelial NOX4$^+$ (A to C, D, and E) staining cells are shown in green (Alexa Fluor-488). Epithelial miR-99b$^+$ (A to C, D, and E) staining cells are shown in red (permanent red substrate). All panels are shown at a magnification of ×40. (F) Quantitation of cells and regions of interest (ROI), which were labeled by an LNA-modified miR-99b probe using Volocity 5.5 software, revealed significantly elevated miR-99b expression in THC/SIV compared to VEH/SIV macaques. Several ROI were hand drawn on the epithelial and LPL regions in the images from duodenum. Image analysis data were analyzed using nonparametric Wilcoxon's rank sum test.

odenum of the THC/SIV macaques (Fig. 4D and E). Quantitative image analysis also provided strong evidence that the duodenal crypt epithelium in the VEH/SIV macaques (Fig. 5A and B) carries a significantly higher number of NOX4$^+$ cells than does that of the THC/SIV macaques (Fig. 5A and B). The presence of a highly conserved predicted miR-99b binding site in the 3′ UTR of NOX4 (TargetScan 6.2) (38) suggested the possibility that elevated miR-99b expression could directly target NOX4 and negatively modulate its protein expression in the intestine. The results of the luciferase reporter assay convincingly demonstrate the latter possibility, i.e., that miR-99b can directly bind to the 3′ UTR of the rhesus macaque NOX4 mRNA and potentially downregulate its protein expression (Fig. 5C). Cotransfection of NOX4-wtUTR and 100 nM miR-99b mimic caused an ~67% reduction in firefly/renilla ratios (Fig. 5C). However, deleting the miR-99b binding sites (NOX4-delUTR) restored firefly/renilla ratios to the level observed with unmanipulated pmirGLO vector (Fig. 5C). In addition, we also quantified lipopolysaccharide binding protein (LBP) levels in plasma to determine if enhanced miR-99b expression correlated with microbial translocation. No significant difference ($P = 0.88$) in LBP levels were detected between VEH/SIV and THC/SIV groups at 60 days p.i (see Fig. S4 in the supplemental material). Surprisingly, one macaque (FT59) in the THC/SIV group had the highest LBP levels in plasma (72 ng/ml) of all macaques. We speculate that the relatively high circulating levels of LBP may be due to the presence of typhlitis secondary to nematode infestation in this animal (Table 1), which could have caused significant disruption of the epithelial barrier. Taken together, these findings suggest that THC-induced miR-99b may contribute to protection of the intestinal epithelium from oxidative stress by downregulating NOX4 expression.

DISCUSSION

Chronic THC administration to SIV-infected macaques reduced plasma viral loads, protected against infection-induced GI inflammation, and prolonged survival (9). More recently, we also demonstrated that chronic THC administration to SIV-infected macaques modulated duodenal T cell populations, stimulated a pro-Th2 cytokine profile, and more importantly, decreased crypt cell

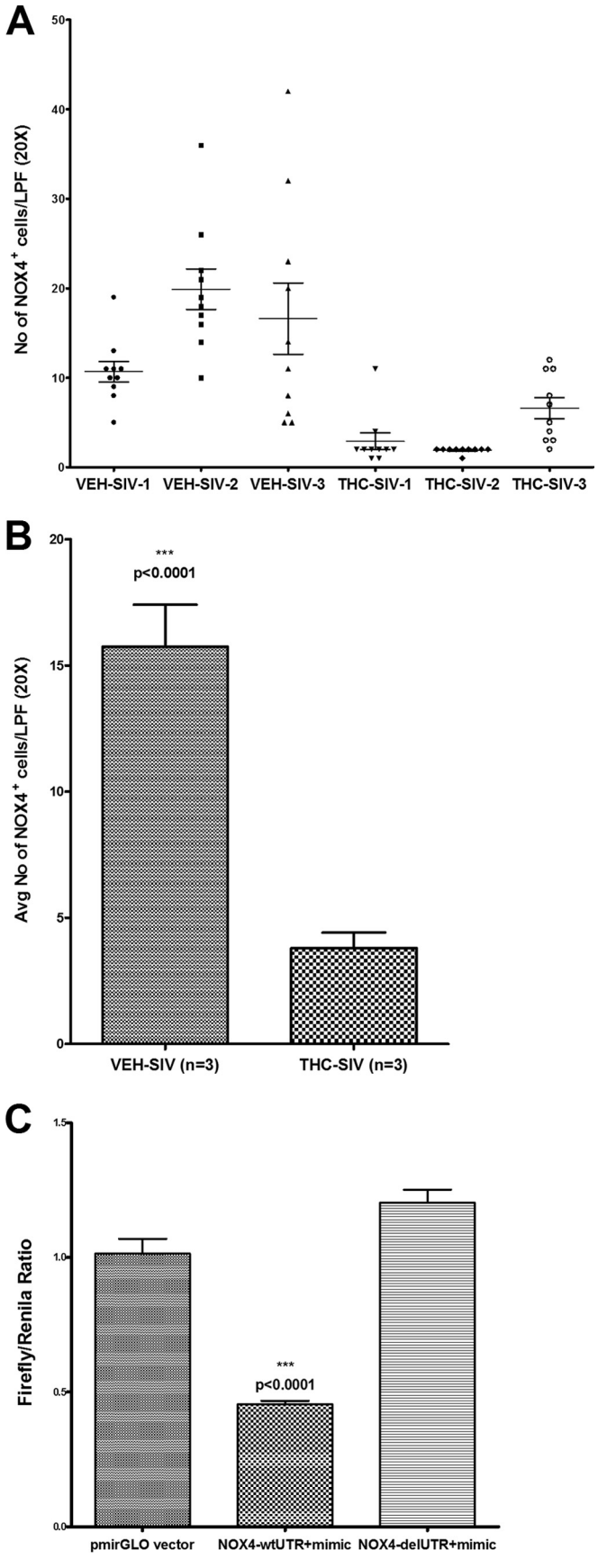

apoptosis in the intestine (21). These findings reveal important modulatory effects of cannabinoids on HIV/SIV disease progression. While some of the proposed mechanisms underlying the immunosuppressive/anti-inflammatory effects of THC include induction of immune cell apoptosis, inhibition of cell proliferation, and suppression of cytokine production, a recent study identified significant upregulation of a specific miRNA, miR-690, in myeloid-derived suppressor cells following THC administration to rats (57). These findings are intriguing and prompted us to investigate whether the anti-inflammatory and apparent protective effects of THC in the intestine involved the differential modulation of miRNA expression. In the present study, we performed miRNA expression profiling in the duodenum of acutely SIV-infected rhesus macaques administered either VEH or THC and identified a THC-induced anti-inflammatory miRNA signature at 60 days p.i. specifically. Among the miRNAs that were notably changed was miR-99b, which directly targets NOX4, a ROS-generating enzyme. In this study, miR-99b expression increased, whereas NOX4 expression decreased significantly in the duodenal epithelium of THC/SIV macaques. Furthermore, chronic THC administration by itself upregulated the expression of a cluster of miRNAs that was identified by a bioinformatics analysis to directly target CXCL12. This chemokine is known to facilitate trafficking of lymphocytes and macrophages into the intestinal lamina propria.

Following OpenArray microRNA profiling, the total number of differentially expressed miRNAs steadily increased from 14 days p.i. to 60 days p.i. in all three groups. Interestingly, almost 80 to 90% of differentially expressed miRNAs in the group that received only THC showed increased expression in the duodenum at all three time points, providing strong evidence that THC positively modulates miRNA expression in the intestine. Most strikingly, at 60 days p.i., ~28% of differentially expressed miRNAs (13/47) in the VEH/SIV group were downregulated compared to the THC/SIV group, in which none of the differentially expressed miRNAs (58) showed decreased expression. Given the recent finding that T cell activation results in global miRNA downregulation, the above finding may indirectly be suggestive of immune activation in the VEH/SIV group and its reduction or attenuation in the THC/SIV group at 60 days p.i. Overall, the data suggest that chronic THC administration positively modulates miRNA expression in both uninfected and SIV-infected macaques and may

FIG 5 (A) Quantification of the number of NOX4$^+$ duodenal crypt epithelial cells from 3 VEH/SIV and 3 THC/SIV macaques. Positive cells were counted at an original magnification of ×20 in a blinded manner in a total of 10 low-power fields (LPF); 1 LPF = 1.1308 mm^2. Each data point represents the number of cells in a single LPF; the error bars represent the mean values. (B) The average number of NOX4$^+$ crypt epithelial cells is higher in the VEH/SIV than in the THC/SIV macaques. Data were analyzed using Wilcoxon's rank sum test. Triple asterisks indicate statistical significance ($P < 0.0001$). (C) miR-99b physically associates with the 3′ UTR of rhesus macaque NOX4 mRNA ($P = 0.0001$). The NOX4 wild-type sequences and those with 3′UTR deleted were inserted into the multiple cloning sites situated in the 3′ end of firefly luciferase gene in the pmirGLO vector. HEK293 cells were cotransfected with 100 nM miR-99b mimic and 100 ng of pmirGLO luciferase reporter constructs containing wild-type (wt) or deleted (del) NOX4 3′UTR sequences. Firefly and renilla luciferase activities were detected using the Dual-Glo luciferase assay system 72 h after transfection. The ratio of luciferase activities (firefly/renilla) was calculated and normalized to the wells transfected with unmanipulated pmirGLO vector. Triple asterisks indicate statistical significance ($P < 0.0001$).

represent a possible mechanism underlying its reported anti-inflammatory/immune activation effects in the intestine.

To identify unique miRNAs that may potentially mediate THC's anti-inflammatory effects, we used a Venn diagram and found the increased expression of at least 9 distinct miRNAs that overlapped between time points. Of these, the expression of 2 (miR-141 and miR-200a) overlapped among all three time points. Interestingly, miR-141 expression was recently shown to be reduced significantly in inflamed colonic epithelial cells from mice with TNBS-induced colitis and from Crohn's disease patients (43). Further, miR-141 downregulation resulted in upregulation of its predicted target, CXCL12β, including total CXCL12 levels (43). Furthermore, transfection of Caco2 cells with premiR-141 prevented lymphocyte migration toward epithelial cells, demonstrating the ability of miR-141 to prevent inflammatory cell migration into the intestinal lamina propria by inhibiting the chemoattractant CXCL12. Intrigued by the above findings, we next scanned the CXCL12 mRNA 3′ UTR using the TargetScan algorithm (38) to determine if predicted binding sites similar to miR-141/miR-200a existed for the other THC-induced miRNAs. Surprisingly, 7 of the 9 THC-induced miRNAs shown in Fig. 1 had one or two predicted binding sites on the 3′ UTR of CXCL12 mRNA (see Tables S4 to S7 in the supplemental material). More interestingly, 5 (miR-141, miR-200a. miR-23a, miR-152, and miR-539) of the 7 miRNAs were predicted to directly target transcript variant 2 coding for the CXCL12β (beta) isoform (accession number NM_000609) (see Table S4 in the supplemental material). Another three miRNAs (miR-23a, miR-301a, and miR-362-3p) have been predicted to directly target transcript variant 1 coding for the CXCL12α (alpha) isoform (accession number NM_199168) (see Table S5 in the supplemental material). At least 2 miRNAs (miR-23a and miR-301a) had predicted binding sites on the 3′ UTR of CXCL12Δ (delta) isoform (NM_001178034) (see Table S6 in the supplemental material). Further, 3 miRNAs (miR-101, miR-29b, and miR-130a) that showed significantly elevated expression in THC/SIV group at 60 days p.i. compared to the VEH/SIV group (Fig. 2D) also had predicted binding sites on all 3 CXCL12 isoforms (miR-101 on CXCL12α, -β, and -Δ; miR-130a on CXCL12α and -Δ; miR-29b on CXCL12β) (see Table S7 in the supplemental material). More interestingly, none of the seven THC-induced miRNAs have been predicted to directly target CXCL12γ (gamma), the specific isoform that has been previously reported to exhibit anti-HIV effects by preventing HIV entry via competitive CXCR4 binding and internalization (59). Consistent with these predictions, cannabinoid agonists (2-AG and JWH-133) have been shown to inhibit CXCL12-mediated chemotaxis of activated T lymphocytes (60). These findings suggest that THC may potentially inhibit inflammatory cell trafficking into the intestinal lamina propria by specifically upregulating the expression of a unique panel of CXCL12-targeting miRNAs. Because the anti-human and -mouse CXCL12 antibodies used in the current study failed to cross-react with the rhesus macaque, it was not possible to determine if levels of CXCL12 protein expression in the intestine differed between the VEH/SIV and THC/SIV macaques.

To identify miRNAs specifically induced by THC in the intestine of SIV-infected macaques, miRNA expression profiles in the duodenum of the THC/SIV and the VEH/SIV groups were compared at the three time points examined. Interestingly, at 60 days p.i., THC was found to selectively upregulate the expression of a group of 19 miRNAs, 6 of which (miR-10a, miR-24, miR-99b, miR-145, miR-149, and miR-187) have been previously identified to target proinflammatory molecules such as cytokines and transcription factors (48–54). Among these, miR-10a was demonstrated to maintain intestinal homeostasis by targeting the proinflammatory cytokine IL-12/IL-23p40 in dendritic cells (DCs) (49). In this study, the authors proposed a mechanism whereby commensal bacteria controlled intestinal inflammation by specifically targeting IL-12/IL-23p40 in DCs (49). Interestingly, mice with lower miR-10a expression showed elevated proinflammatory cytokine expression. However, inhibition of miR-10a function using specific antagomirs significantly promoted IL-12 production in DCs, providing further support for the anti-inflammatory properties of miR-10a (49). In a separate study involving atherosclerosis-susceptible endothelium, miR-10a expression was found to be downregulated and the expression of its predicted target HOXA1 was significantly upregulated (50). Likewise, miR-24 expression significantly increased in the inflamed colons of pediatric inflammatory bowel disease (IBD) patients, suggesting that the upregulation may be a host response to curtail inflammatory signaling (51). Similarly, IL-10 was reported to suppress production of proinflammatory cytokines such as TNF-α, IL-6, and IL-12 by selectively inducing the upregulation of miR-187 (48). Further, miR-187 inhibited TNF-α production by directly binding to the 3′ UTR of TNF-α mRNA and downregulating its expression (48). In addition, overexpression of miR-187 significantly reduced TNF-α, IL-6, and IL-12p40 production in LPS-activated monocytes (48). Nevertheless, these anti-inflammatory effects were reversed when miR-187 was silenced using antagomirs (48). Along similar lines, expression of the anti-inflammatory miR-145 decreased markedly in the colons of ulcerative colitis patients (53). In addition, decreased expression of miR-145 resulted in elevated expression of its predicted target Insulin Receptor Substrate 1 (IRS-1) (53). Additionally, overexpression of miR-145 in HCT116 cells significantly decreased the IRS-1 expression. In HUVEC and Eahy926 cell lines, miR-149 prevented endothelial dysfunction by blocking TNF-α-induced MMP-9 expression (54). As mentioned earlier, significant increases in IL-6, IL-12, and IL-1β production occurred following miR-99b knockdown in DCs, suggesting its strong anti-inflammatory function (49). It is also interesting that the induction of anti-inflammatory miRNAs in the THC/SIV group was not detectable until 60 days p.i., suggesting that alternative mechanisms may be involved in THC-mediated protective effects during early infection. These may involve histone modifications, another important epigenetic mechanism regulating proinflammatory gene transcription. Additional mechanisms may involve the early induction of anti-inflammatory cytokines such as IL-10 and T regulatory cells.

To determine the functional significance of miR-99b upregulation in the THC/SIV group specifically, we next focused on NOX4, a predicted miR-99b target and a major generator of ROS in epithelial cells (54, 55). Further, based on *in situ* hybridization studies, miR-99b was found to be predominantly localized to the duodenal epithelium of both VEH/SIV- and THC/SIV-infected macaques. Interestingly, a significant increase in the number of $NOX4^{+}$ crypt epithelial cells was detected in the VEH/SIV group compared to the THC/SIV group. Luciferase reporter assays provided strong evidence that NOX4 can be directly targeted by miR-99b through binding to its 3′ UTR, resulting in its reduced expression in the intestine of THC/SIV macaques. In contrast, decreased

miR-99b expression, as revealed by qRT-PCR (Fig. 3C) in the intestines of VEH/SIV macaques, was accompanied by an increased number of NOX4$^+$ crypt epithelial cells (Fig. 4A and B). These findings show that THC could exert protection from SIV disease progression by selectively modulating the expression of a panel of miRNAs with anti-inflammatory functions. More importantly, miR-99b-mediated downregulation of NOX4 represents a potential epigenetic mechanism by which THC protects the intestinal epithelium against oxidative stress, as NOX4 expression in epithelial cells has been reported to result in constitutive ROS production mainly on internal membranes (56, 58). In addition to miR-99b, NOX4 can also be targeted by other miRNAs, and its expression can be regulated by other epigenetic mechanisms such as histone modifications. Because lipopolysaccharide (LPS) has been shown to reduce colonic epithelial cell viability by inducing NOX-dependent ROS generation (56), the increased number of NOX4$^+$ enterocytes in the VEH/SIV macaques indicates the activation of epithelial cells by oxidative stress (61) or possibly by luminal bacteria and their products acting via Toll-like receptor 4 (TLR4) (62). Accordingly, uncontrolled oxidative stress resulting from NOX4 hyperactivity can lead to epithelial cell apoptosis/death (54, 63), causing disruption of the epithelial barrier, microbial translocation, systemic immune activation, and HIV/SIV disease progression.

In summary, the present study provides novel information on the epigenetic effects of Δ^9-THC, particularly via anti-inflammatory miRNA induction in the intestine of uninfected and SIV-infected macaques. We previously showed that THC administration protected the intestine epithelium against infection/inflammation-induced cell death in chronically SIV-infected rhesus macaques. In the present study, we show that THC may exert similar protective effects on the intestinal epithelium from acute infection-induced inflammation and cell death by modulating the expression of anti-inflammatory miRNAs during acute SIV infection. Among the several miRNAs, we show that miR-99b, by mediating downregulation of NOX4, could protect the intestinal epithelium from the damaging effects of oxidative stress.

While we have identified several THC-induced anti-inflammatory miRNAs, future studies are needed to determine the specific mucosal compartment (epithelial versus lamina propria) contributing to the upregulation. While cannabinoid-activated signaling in the brain is transduced primarily via the CB1 receptor (64), the anti-inflammatory effects of THC in the GI tract are mediated predominantly via increased CB2 receptor expression (18, 19). In this regard, future studies using CB2-blocking agents such as antibodies or small molecule inhibitors/antagonists are needed to determine if miR-99b-mediated NOX4 downregulation is a direct or indirect effect of THC. Another important and interesting finding in the present study was that THC administration to uninfected and SIV-infected macaques positively regulated the expression of several miRNAs that have been predicted by bioinformatics to target CXCL12. Future studies are also needed to confirm whether THC administration negatively impacts CXCL12 protein expression, as this chemokine plays a critical role in the trafficking of inflammatory cells into the intestinal lamina propria. The possible reduction of inflammation by THC-induced miRNAs warrants further investigation in other target organs and is currently the focus of ongoing investigations.

ACKNOWLEDGMENTS

This study was supported by National Institutes of Health grants R01DA030053 to P.M., R01DK083929 to M.M., P60AA09803 (Analytical Core Laboratory LSUHSC Alcohol Research Center), and OD011104 (formerly RR00164).

We thank Ronald S. Veazey, Andrew A. Lackner, Xavier Alvarez, Maurice Duplantis, Yun Te Lin, Faith R. Schiro, Cecily C. Midkiff, Connie Poretta, and Robin Rodriguez for their technical assistance in the study and Robert Siggins for discussions on flow cytometry results.

REFERENCES

1. **Haney M, Gunderson EW, Rabkin J, Hart CL, Vosburg SK, Comer SD, Foltin RW.** 2007. Dronabinol and marijuana in HIV-positive marijuana smokers. Caloric intake, mood, and sleep. J Acquir Immune Defic Syndr **45:**545–554. http://dx.doi.org/10.1097/QAI.0b013e31811ed205.
2. **Riggs PK, Vaida F, Rossi SS, Sorkin LS, Gouaux B, Grant I, Ellis RJ.** 2012. A pilot study of the effects of cannabis on appetite hormones in HIV-infected adult men. Brain Res **1431:**46–52. http://dx.doi.org/10.1016/j.brainres.2011.11.001.
3. **Tambaro S, Casu MA, Mastinu A, Lazzari P.** 2014. Evaluation of selective cannabinoid CB1 and CB2 receptor agonists in a mouse model of lipopolysaccharide-induced interstitial cystitis. 2014. Eur J Pharmacol **729:**67–74. http://dx.doi.org/10.1016/j.ejphar.2014.02.013.
4. **Kaplan BL.** 2013. The role of CB1 in immune modulation by cannabinoids. Pharmacol Ther **137:**365–374. http://dx.doi.org/10.1016/j.pharmthera.2012.12.004.
5. **Rom S, Persidsky Y.** 2013. Cannabinoid receptor2: potential role in immunomodulation and neuroinflammation. J Neuroimmune Pharmacol **8:**608–620. http://dx.doi.org/10.1007/s11481-013-9445-9.
6. **Harvey BS, Nicotra LL, Vu M, Smid SD.** 2013. Cannabinoid CB2 receptor activation attenuates cytokine-evoked mucosal damage in a human colonic explant model without changing epithelial permeability. Cytokine **63:**209–217. http://dx.doi.org/10.1016/j.cyto.2013.04.032.
7. **Mukhopadhyay P, Rajesh M, Pan H, Patel V, Mukhopadhyay B, Bátkai S, Gao B, Haskó G, Pacher P.** 2010. Cannabinoid-2 receptor limits inflammation, oxidative/nitrosative stress, and cell death in nephropathy. Free Radic Biol Med **48:**457–467. http://dx.doi.org/10.1016/j.freeradbiomed.2009.11.022.
8. **Dunn SL, Wilkinson JM, Crawford A, Le Maitre CL, Bunning RA.** 2012. Cannabinoids: novel therapies for arthritis? Future Med Chem **4:**713–725. http://dx.doi.org/10.4155/fmc.12.20.
9. **Molina PE, Winsauer P, Zhang P, Walker E, Birke L, Amedee A, Stouwe CV, Troxclair D, McGoey R, Varner K, Byerley L, LaMotte L.** 2011. Cannabinoid administration attenuates the progression of simian immunodeficiency virus. AIDS Res Hum Retroviruses **27:**585–592. http://dx.doi.org/10.1089/aid.2010.0218.
10. **Winsauer PJ, Molina PE, Amedee AM, Filipeanu CM, McGoey RR, Troxclair DA, Walker EM, Birke LL, Stouwe CV, Howard JM, Leonard ST, Moerschbaecher JM, Lewis PB.** 2011. Tolerance to chronic delta-9-tetrahydrocannabinol (Δ^9-THC) in rhesus macaques infected with simian immunodeficiency virus. Exp Clin Psychopharmacol **19:**154–172. http://dx.doi.org/10.1037/a0023000.
11. **Molina PE, Amedee A, LeCapitaine NJ, Zabaleta J, Mohan M, Winsauer P, Vande Stouwe C.** 2011. Cannabinoid neuroimmune modulation of SIV disease. J Neuroimmune Pharmacol **6:**516–527. http://dx.doi.org/10.1007/s11481-011-9301-8.
12. **Lackner AA, Mohan M, Veazey RS.** 2009. The gastrointestinal tract and AIDS pathogenesis. Gastroenterology **136:**1965–1978. http://dx.doi.org/10.1053/j.gastro.2008.12.071.
13. **Veazey RS, DeMaria M, Chalifoux LV, Shvetz DE, Pauley DR, Knight HL, Rosenzweig M, Johnson RP, Desrosiers RC, Lackner AA.** 1998. Gastrointestinal tract as a major site of CD4$^+$ T cell depletion and viral replication in SIV infection. Science **280:**427–431. http://dx.doi.org/10.1126/science.280.5362.427.
14. **Smit-McBride Z, Mattapallil JJ, McChesney M, Ferrick D, Dandekar S.** 1998. Gastrointestinal T lymphocytes retain high potential for cytokine responses but have severe CD4(+) T-cell depletion at all stages of simian immunodeficiency virus infection compared to peripheral lymphocytes. J Virol **72:**6646–6656.
15. **Mehandru S, Poles MA, Tenner-Racz K, Horowitz A, Hurley A, Hogan C, Boden D, Racz P, Markowitz M.** 2004. Primary HIV-1 infection is

associated with preferential depletion of $CD4^+$ T lymphocytes from effector sites in the gastrointestinal tract. J Exp Med **200:**761–770. http://dx.doi.org/10.1084/jem.20041196.
16. **Sankaran S, George MD, Reay E, Guadalupe M, Flamm J, Prindiville T, Dandekar S.** 2008. Rapid onset of intestinal epithelial barrier dysfunction in primary human immunodeficiency virus infection is driven by an imbalance between immune response and mucosal repair and regeneration. J Virol **82:**538–545. http://dx.doi.org/10.1128/JVI.01449-07.
17. **Mohan M, Aye PP, Borda J T, Alvarez X, Lackner AA.** 2007. Gastrointestinal disease in simian immunodeficiency virus-infected rhesus macaques is characterized by proinflammatory dysregulation of the interleukin-6-janus kinase/signal transducer and activator of transcription-3 pathway. Am J Pathol **171:**1952–1965. http://dx.doi.org/10.2353/ajpath.2007.070017.
18. **Mohan M, Kaushal D, Aye PP, Alvarez X, Veazey RS, Lackner AA.** 2012. Focused examination of the intestinal lamina propria yields greater molecular insight into mechanisms underlying SIV induced immune dysfunction. PLoS One **7**(4):e34561. http://dx.doi.org/10.1371/journal.pone.0034561.
19. **Marchetti G, Tincati C, Silvestri G.** 2013. Microbial translocation in the pathogenesis of HIV infection and AIDS. Clin Microbiol Rev **26:**2–18. http://dx.doi.org/10.1128/CMR.00050-12.
20. **Wright KL, Duncan M, Sharkey KA.** 2008. Cannabinoid CB2 receptors in the gastrointestinal tract: a regulatory system in states of inflammation. Br J Pharmacol **153:**263–270. http://dx.doi.org/10.1038/sj.bjp.0707486.
21. **Esposito G, Filippis DD, Cirillo C, Iuvone T, Capoccia E, Scuderi C, Steardo A, Cuomo R, Steardo L.** 2013. 2013. Cannabidiol in inflammatory bowel diseases: a brief overview. Phytother Res **27:**633–636. http://dx.doi.org/10.1002/ptr.4781.
22. **Naftali T, Bar-Lev Schleider L, Dotan I, Lansky EP, Sklerovsky Benjaminov F, Konikoff FM.** 2013. Cannabis induces a clinical response in patients with Crohn's disease: a prospective placebo-controlled study. Clin Gastroenterol Hepatol **11:**1276–1280. http://dx.doi.org/10.1016/j.cgh.2013.04.034.
23. **Molina PE, Amedee AM, Lecapitaine NJ, Zabaleta J, Mohan M, Winsauer PJ, Vande Stouwe C, McGoey RR, Auten MW, Lamotte L, Chandra LC, Birke LL.** 2014. Modulation of gut-specific mechanisms by chronic Δ^9-tetrahydrocannabinol administration in male rhesus macaques infected with simian immunodeficiency virus: a systems biology analysis. AIDS Res Hum Retroviruses **30:**567–578. http://dx.doi.org/10.1089/aid.2013.0182.
24. **Ramirez SH, Reichenbach NL, Fan S, Rom S, Merkel SF, Wang X, Ho WZ, Persidsky Y.** 2013. Attenuation of HIV-1 replication in macrophages by cannabinoid receptor 2 agonists. J Leukoc Biol **93:**801–810. http://dx.doi.org/10.1189/jlb.1012523.
25. **Jonkman S, Kenny PJ.** 2013. Molecular, cellular, and structural mechanisms of cocaine addiction: a key role for microRNAs. Neuropsychopharmacology **38:**198–211. http://dx.doi.org/10.1038/npp.2012.120.
26. **Rodríguez RE.** 2012. Morphine and microRNA activity: is there a relation with addiction? Front Genet **3:**223. http://dx.doi.org/10.3389/fgene.2012.00223.
27. **Hu G, Yao H, Chaudhuri AD, Duan M, Yelamanchili SV, Wen H, Cheney PD, Fox HS, Buch S.** 2012. Exosome-mediated shuttling of microRNA-29 regulates HIV Tat and morphine-mediated neuronal dysfunction. Cell Death Dis **3:**e381. http://dx.doi.org/10.1038/cddis.2012.114.
28. **He Y, Wang ZJ.** 2012. Let-7 microRNAs and opioid tolerance. Front Genet **21:**110. http://dx.doi.org/10.3389/fgene.2012.00110.
29. **Li J, Li J, Liu X, Qin S, Guan Y, Liu Y, Cheng Y, Chen X, Li W, Wang S, Xiong M, Kuzhikandathil EV, Ye JH, Zhang C.** 2013. MicroRNA expression profile and functional analysis reveal that miR-382 is a critical novel gene of alcohol addiction. EMBO Mol Med **5:**1402–1414. http://dx.doi.org/10.1002/emmm.201201900.
30. **Sun G, Li H, Wu X, Covarrubias M, Scherer L, Meinking K, Luk B, Chomchan P, Alluin J, Gombart AF, Rossi JJ.** 2012. Interplay between HIV-1 infection and host microRNAs. Nucleic Acids Res **40:**2181–2196. http://dx.doi.org/10.1093/nar/gkr961.
31. **Duskova K, Nagilla P, Le HS, Iyer P, Thalamuthu A, Martinson J, Bar-Joseph Z, Buchanan W, Rinaldo C, Ayyavoo V.** 2013. MicroRNA regulation and its effects on cellular transcriptome in human immunodeficiency virus-1 (HIV-1) infected individuals with distinct viral load and CD4 cell counts. BMC Infect Dis **13:**250. http://dx.doi.org/10.1186/1471-2334-13-250.
32. **Swaminathan S, Hu X, Zheng X, Kriga Y, Shetty J, Zhao Y, Stephens R, Tran B, Baseler MW, Yang J, Lempicki RA, Huang D, Lane HC, Imamichi T.** 2013. Interleukin-27 treated human macrophages induce the expression of novel microRNAs which may mediate anti-viral properties. Biochem Biophys Res Commun **434:**228–234. http://dx.doi.org/10.1016/j.bbrc.2013.03.046.
33. **Chiang K, Liu H, Rice AP.** 2013. miR-132 enhances HIV-1 replication. Virology **438:**1–4. http://dx.doi.org/10.1016/j.virol.2012.12.016.
34. **Swaminathan S, Suzuki K, Seddiki N, Kaplan W, Cowley MJ, Hood CL, Clancy J L, Murray DD, Méndez C, Gelgor L, Anderson B, Roth N, Cooper DA, Kelleher AD.** 2012. Differential regulation of the Let-7 family of microRNAs in CD4+ T cells alters IL-10 expression. J Immunol **188:**6238–6246. http://dx.doi.org/10.4049/jimmunol.1101196.
35. **Yelamanchili SV, Chaudhuri AD, Chen LN, Xiong H, Fox HS.** 2010. MicroRNA-21 dysregulates the expression of MEF2C in neurons in monkey and human SIV/HIV neurological disease. Cell Death Dis **1:**e77. http://dx.doi.org/10.1038/cddis.2010.56.
36. **Witwer KW, Sarbanes SL, Liu J, Clements JE.** 2011. A plasma microRNA signature of acute lentiviral infection: biomarkers of central nervous system disease. AIDS **25:**2057–2067. http://dx.doi.org/10.1097/QAD.0b013e32834b95bf.
37. **Mohan M, Chandra LC, Aye PP, Alvarez X, Lackner AA.** 2014. miR-190b is markedly upregulated in the intestine in response to SIV replication and partly regulates myotubularin related protein-6 expression. J Immunol **193:**1301–1313. http://dx.doi.org/10.4049/jimmunol.1303479.
38. **Lewis BP, Burge CB, Bartel DP.** 2005. Conserved seed pairing, often flanked by adenosines, indicates that thousands of human genes are microRNA targets. Cell **120:**15–20. http://dx.doi.org/10.1016/j.cell.2004.12.035.
39. **Wu H, Neilson JR, Kumar P, Manocha M, Shankar P, Sharp PA, Manjunath N.** 2007. miRNA profiling of naïve, effector and memory CD8 T cells. PLoS One **2**(10):e1020. http://dx.doi.org/10.1371/journal.pone.0001020.
40. **Bronevetsky Y, Villarino AV, Eisley CJ, Barbeau R, Barczak AJ, Heinz GA, Kremmer E, Heissmeyer V, McManus MT, Erle DJ, Rao A, Ansel KM.** 2013. T cell activation induces proteasomal degradation of Argonaute and rapid remodeling of the microRNA repertoire. J Exp Med **210:**417–432. http://dx.doi.org/10.1084/jem.20111717.
41. **Jeker LT, Bluestone JA.** 2013. MicroRNA regulation of T-cell differentiation and function. Immunol Rev **253:**65–81. http://dx.doi.org/10.1111/imr.12061.
42. **Trifari S, Pipkin ME, Bandukwala HS, Äijö T, Bassein J, Chen R, Martinez GJ, Rao A.** 2013. MicroRNA-directed program of cytotoxic CD8+ T-cell differentiation. Proc Natl Acad Sci U S A **110:**18608–18613. http://dx.doi.org/10.1073/pnas.1317191110.
43. **Huang Z, Shi T, Zhou Q, Shi S, Zhao R, Shi H, Dong L, Zhang C, Zeng K, Chen J, Zhang J.** 2014. miR-141 Regulates colonic leukocytic trafficking by targeting CXCL12β during murine colitis and human Crohn's disease. Gut **63:**1247–1257. http://dx.doi.org/10.1136/gutjnl-2012-304213.
44. **John B, Enright AJ, Aravin A, Tuschl T, Sander C, Marks DS.** 2005. Human microRNA targets. PLoS Biol **3**(7):e264. http://dx.doi.org/10.1371/journal.pbio.0030264.
45. **Dotan I, Werner L, Vigodman S, Weiss S, Brazowski E, Maharshak N, Chen O, Tulchinsky H, Halpern Z, Guzner-Gur H.** 2010. CXCL12 is a constitutive and inflammatory chemokine in the intestinal immune system. Inflamm Bowel Dis **16:**583–592. http://dx.doi.org/10.1002/ibd.21106.
46. **Werner L, Guzner-Gur H, Dotan I.** 2013. Involvement of CXCR4/CXCR7/CXCL12 interactions in inflammatory bowel disease. Theranostics **3:**40–46. http://dx.doi.org/10.7150/thno.5135.
47. **Zhao H, Anand AR, Ganju RK.** 2014. Slit2-Robo4 pathway modulates lipopolysaccharide-induced endothelial inflammation and its expression is dysregulated during endotoxemia. J Immunol **192:**385–393. http://dx.doi.org/10.4049/jimmunol.1302021.
48. **Rossato M, Curtale G, Tamassia N, Castellucci M, Mori L, Gasperini S, Mariotti B, De Luca M, Mirolo M, Cassatella MA, Locati M, Bazzoni F.** 2012. IL-10-induced microRNA-187 negatively regulates TNF-α, IL-6, and IL-12p40 production in TLR4-stimulated monocytes. Proc Natl Acad Sci U S A **109:**E3101–E3110. http://dx.doi.org/10.1073/pnas.1209100109.
49. **Xue X, Feng T, Yao S, Wolf KJ, Liu CG, Liu X, Elson CO, Cong Y.** 2011. Microbiota downregulates dendritic cell expression of miR-10a, which targets IL-12/IL-23p40. J Immunol **187:**5879–5886. http://dx.doi.org/10.4049/jimmunol.1100535.

50. **Fang Y, Shi C, Manduchi E, Civelek M, Davies PF.** 2010. MicroRNA-10a regulation of proinflammatory phenotype in athero-susceptible endothelium in vivo and in vitro. Proc Natl Acad Sci U S A **107:**13450–13455. http://dx.doi.org/10.1073/pnas.1002120107.
51. **Zahm AM, Hand NJ, Tsoucas DM, Le Guen CL, Baldassano RN, Friedman JR.** 2014. Rectal microRNAs are perturbed in pediatric inflammatory bowel disease of the colon. J Crohns Colitis **8:**1108–1117. http://dx.doi.org/10.1016/j.crohns.2014.02.012.
52. **Singh Y, Kaul V, Mehra A, Chatterjee S, Tousif S, Dwivedi VP, Suar M, Van Kaer L, Bishai WR, Das G.** 2013. *Mycobacterium tuberculosis* controls microRNA-99b (miR-99b) expression in infected murine dendritic cells to modulate host immunity. J Biol Chem **288:**5056–5061. http://dx.doi.org/10.1074/jbc.C112.439778.
53. **Pekow JR, Dougherty U, Mustafi R, Zhu H, Kocherginsky M, Rubin DT, Hanauer SB, Hart J, Chang EB, Fichera A, Joseph LJ, Bissonnette M.** 2012. miR-143 and miR-145 are downregulated in ulcerative colitis: putative regulators of inflammation and protooncogenes. Inflamm Bowel Dis **18:**94–100. http://dx.doi.org/10.1002/ibd.21742.
54. **Palmieri D, Capponi S, Geroldi A, Mura M, Mandich P, Palombo D.** 2014. TNFα induces the expression of genes associated with endothelial dysfunction through p38MAPK-mediated down-regulation of miR-149. Biochem Biophys Res Commun **443:**246–251. http://dx.doi.org/10.1016/j.bbrc.2013.11.092.
55. **Dalmasso G, Nguyen HT, Yan Y, Laroui H, Srinivasan S, Sitaraman SV, Merlin D.** 2010. MicroRNAs determine human intestinal epithelial cell fate. Differentiation **80:**147–154. http://dx.doi.org/10.1016/j.diff.2010.06.005.
56. **Ramonaite R, Skieceviciene J, Kiudelis G, Jonaitis L, Tamelis A, Cizas P, Borutaite V, Kupcinskas L.** 2013. Influence of NADPH oxidase on inflammatory response in primary intestinal epithelial cells in patients with ulcerative colitis. BMC Gastroenterol **13:**159. http://dx.doi.org/10.1186/1471-230X-13-159.
57. **Hegde VL, Tomar S, Jackson A, Rao R, Yang X, Singh UP, Singh NP, Nagarkatti PS, Nagarkatti M.** 2013. Distinct microRNA expression profile and targeted biological pathways in functional myeloid-derived suppressor cells induced by Δ9-tetrahydrocannabinol in vivo: regulation of CCAAT/enhancer-binding protein α by microRNA-690. J Biol Chem **288:**36810–36826. http://dx.doi.org/10.1074/jbc.M113.503037.
58. **Martyn KD, Frederick LM, von Loehneysen K, Dinauer MC, Knaus UG.** 2006. Functional analysis of Nox4 reveals unique characteristics compared to other NADPH oxidases. Cell Signal **18:**69–82. http://dx.doi.org/10.1016/j.cellsig.2005.03.023.
59. **Altenburg JD, Jin Q, Alkhatib B, Alkhatib G.** 2010. The potent anti-HIV activity of CXCL12gamma correlates with efficient CXCR4 binding and internalization. J Virol **84:**2563–2572. http://dx.doi.org/10.1128/JVI.00342-09.
60. **Coopman K, Smith LD, Wright KL, Ward SG.** 2007. Temporal variation in CB2R levels following T lymphocyte activation: evidence that cannabinoids modulate CXCL12-induced chemotaxis. Int Immunopharmacol **7:**360–371. http://dx.doi.org/10.1016/j.intimp.2006.11.008.
61. **Dolowschiak T, Chassin C, Ben Mkaddem S, Fuchs TM, Weiss S, Vandewalle A, Hornef MW.** 2010. Potentiation of epithelial innate host responses by intercellular communication. PLoS Pathog **6**(11):e1001194. http://dx.doi.org/10.1371/journal.ppat.1001194.
62. **Park HS, Jung HY, Park EY, Kim J, Lee WJ, Bae YS.** 2004. Cutting edge: direct interaction of TLR4 with NAD(P)H oxidase 4 isozyme is essential for lipopolysaccharide-induced production of reactive oxygen species and activation of NF-kappa B. J Immunol **173:**3589–3593. http://dx.doi.org/10.4049/jimmunol.173.6.3589.
63. **Carnesecchi S, Deffert C, Donati Y, Basset O, Hinz B, Preynat-Seauve O, Guichard C, Arbiser JL, Banfi B, Pache JC, Barazzone-Argiroffo C, Krause KH.** 2011. A key role for NOX4 in epithelial cell death during development of lung fibrosis. Antioxid Redox Signal **15:**607–619. http://dx.doi.org/10.1089/ars.2010.3829.
64. **Devinsky O, Cilio MR, Cross H, Fernandez-Ruiz J, French J, Hill C, Katz R, Di Marzo V, Jutras-Aswad D, Notcutt WG, Martinez-Orgado J, Robson PJ, Rohrback BG, Thiele E, Whalley B, Friedman D.** 2014. Cannabidiol: pharmacology and potential therapeutic role in epilepsy and other neuropsychiatric disorders. Epilepsia **55:**791–802. http://dx.doi.org/10.1111/epi.12631.